Desalination and Water Treatment
www.deswater.com
doi: 10.1080/19443994.2014.930700

55 (2015) 2034–2043
August

Taylor & Francis
Taylor & Francis Group

Application of an integrated system of coagulation and electrodialysis for treatment of wastewater produced by fracturing

Huawei Hao[a,b], Xing Huang[a,b], Congjie Gao[a,b], Xueli Gao[a,b,*]

[a]*Key Laboratory of Marine Chemistry Theory and Technology, Ministry of Education, Qingdao 266100, Shandong, China, Tel./Fax: +86 0532 66782017; emails: haohuawei_ouc@163.com (H. Hao), qinmengyunxiao@126.com (X. Huang), gaocjie@ouc.edu.cn (C. Gao), gxl_ouc@126.com (X. Gao)*
[b]*College of Chemistry & Chemical Engineering, Ocean University of China, Qingdao 266100, Shandong, China*

Received 17 November 2013; Accepted 28 May 2014

ABSTRACT

In order to produce large quantities of newly discovered unconventional oil and gas, hydraulic fracturing of wells is commonly practiced in the oilfields. While the "Frac jobs" for shale gas are completed, tremendous water will flow back to the surface, and then fracturing wastewater is generated. In this study, an integrated process consisting of coagulation and electrodialysis (ED) is proposed to treat the fracturing wastewater. The coagulation is used to remove the organic contaminants and purify the water. The chemical oxygen demand and turbidity is recorded before and after experiment in order to monitor the coagulant effect. In the ED system, the ion-removal efficiency is studied to measure the desalinating effect. The removal rate of ions reach up to 91%, except that the removal rate of SO_4^{2-} is 84.3%, and the product water can basically meet the requirements of wastewater reclamation. After the experiments, the membrane fouling is inspected through electron microscopy and static contact angle. The fouling deposits on the surface of cation exchange membrane and anion exchange membrane are not visibly observed. It is proved that the ED process for deep desalination is suitable for a long-term operation.

Keywords: Fracturing wastewater; Coagulation; Electrodialysis; Deep desalination

1. Introduction

Since the fracturing technology is proved to be extremely effective and applicable for achieving stable production and improving productivity [1–3], the fracturing technology is extensively applied in China and other countries around the world. Water is, by far, the most common fracturing fluid—96% of all fractured wells employ an aqueous fluid. "Frac jobs" for shale gas production in the Marcellus basin, for example, requires about 3.8 million liters of water for vertical wells and 11–22 million liters for horizontal wells [4]. Inevitably, oil and gas production processes generate huge amounts of fracturing wastewater. Because oil and gas wastewater contains massive organic and inorganic contaminants, such as Guanidine gum, formaldehyde, oil, and high mineral ions; the wastewater is characterized with high chemical oxygen demand (COD), high stability, and high salinity. If discharged directly, massive wastewater can pollute the environment seriously, especially the groundwater, soil, and crops [5]. What is worse, the fracturing

*Corresponding author.

wastewater cannot be reclaimed efficiently due to that ions tend to scaling and plugging system of pipelines. Therefore, fracturing wastewater treatment is an urgent problem to be solved.

Current management techniques for fracturing wastewater include discharge, deep-well injection, and treatment [6–8]. Considering environmental impacts of drilling and hydraulic fracturing of wells, China is enforcing more stringent regulation and discharge limits on the oil and gas companies. In that way, directly discharging fracturing wastewater is impracticable and illegal now. Deep-well injection of fracturing wastewater is adopted worldwide as a practice for waste disposal. After the liquid wastes are injected, the performance of injection wells during the deep-well injection of liquid wastes critically depends upon the physical–chemical properties of the waste and operational parameters such as injection rates and pressures, as well as the hydrogeological and geochemical characteristics of the host formation [9,10]. However, the long-term influence of underground injection of oil and gas waste is not well understood, and this method permanently removes water away from the natural fresh water recycle. Conventional treatment methods allow 50–60% water recovery, but minute suspended oil and hazardous dissolved organic/inorganic contaminants are still contained in the product water [11–13]. To solve the above problems, an integrated process consisting of coagulation and electrodialysis (ED), which has been rarely reported previously, is introduced in this paper.

Coagulation is used to remove the organic and inorganic contaminants, such as suspended particles, phosphates, and insoluble free hydrocarbons. Comparing with alternative treatments, coagulation is a cost-effective and efficient technology to remove color, COD, and the turbidity [14]. A large quantity of coagulants, for example, inorganic salts of aluminum chloride, aluminum sulfate, and polyaluminum chloride (PAC), are commercially available and widely used as reactants in coagulation system [15]. In a study, Sher et al. [16] used the coagulation process to purify the effluent from a polymer plant by effectively removing the COD and turbidity up to 99 and 99.8%, respectively. ED is an electrochemical separation process with ion-exchange membranes using an electric potential as the driving force to separate and purify ionic species. Due to its inherent advantages such as environmental friendliness, convenience of operation, and low-energy consumption, ED has been widely applied in many fields [17]. ED consists of dilute and concentrate compartments with alternating cation and anion exchange membranes (AEMs) in a stack. When a continuous direct current (DC) is established, cations are preferentially transported through cation exchange membranes (CEMs) and anions through (AEMs) [18]. Consequently, ions are accumulated in a concentrate compartment and are depleted in the dilute compartment simultaneously. In this paper, the specific objectives of this study were: (a) optimization of ED processes for fracturing wastewater and (b) improvement of removal efficiency of ions from the feeding solution.

2. Materials and methods

2.1. Reagent and materials

PAC and polyacrylamide (PAM) were of analytical grade and used as coagulation and coagulation aid without further purification in the pretreatment system, respectively. The fracturing wastewater was collected from the Shengli Oilfield, Dongying city, Shandong Province, China. The main characteristics of fracturing wastewater are shown in Table 1. The CEM and AEM were supplied by Qianqiu Environmental Protection & Water Treatment Corporation and their main characteristics are detailed in Table 2.

2.2. Apparatus

The flow chart for the whole apparatus is presented in Fig. 1. The coagulation–flocculation is included in the integrated process. ED device has three separated circuits developed by three peristaltic pumps (ZG-60-500 Boding Longer Peristaltic Pump Ltd.) with three rotameters (0–25 L/h) and three 5 L

Table 1
The main characteristics of fracturing wastewater

Parameter	Unit	Fracturing wastewater
pH		7.0
Petroleum	mg/L	104
COD[a]	mg/L	10,873
Turbidity	NTU	>2,000
BOD_5[b]	mg/L	5,477
Suspended solids	mg/L	80
Total alkalinity	mg/L	1,015
Conductivity	ms/cm	22.4
Chloride	mg/L	6,892
Nitrate	mg/L	6.3
Sulfate	mg/L	535
Calcium	mg/L	174
Magnesium	mg/L	21.7
Sodium	mg/L	6,055

[a]COD: chemical oxygen demand.
[b]BOD_5: biochemical oxygen demand at 5 d.

Table 2
The main characteristics of the ion-exchange membranes

Membrane	Thickness (mm)	IEC ($meqg^{-1}$)	Area resistance (Ωcm^2)	Selectivity
AEM	0.6	1.8	15	>92%
CEM	0.8	2.0	18	>94%

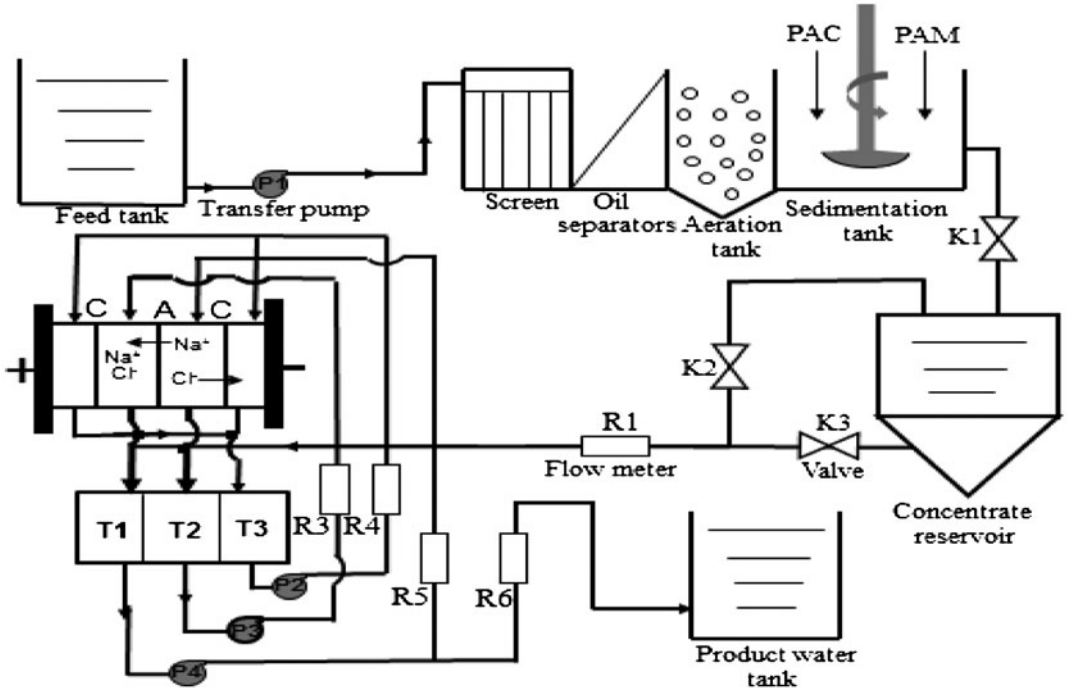

Fig. 1. Flow chart of treatment and reclamation of fracturing wastewater; T1—tank for concentrated solution; T2—tank for dilute solution and T3—tank for electrode solution.

tanks for the dilute solution, the concentrated solution, and the electrode solution. There are 10 cell pairs membrane in the stack and the effective surface area of each membrane was 162 cm^2. In this experiment, the product water from the pretreatment is utilized as dilute and concentrated streams in ED. Sodium sulfate (0.5 mol/L) is utilized as the electrode solution.

2.3. Experimental procedure

Bench-scale tests were mainly performed to investigate the technological parameters of the integrated process. The coagulation–flocculation experiments were carried out in the 150 mL breakers. The solution pH was always nearby 7.0 and the standing time was fixed at 90 min in all cases. Once the standing time and pH had been established, the remaining variables were also determined by the experiments as follows: the coagulant was added with a dosage varying from 0 to 500 $mg\,L^{-1}$ and coagulant aid was added with a dosage varying from 0 to 8 $mg\,L^{-1}$. Finally, the influence of standing time on the height of the clarification zone was also studied [19]. In the experiment, COD and turbidity were mainly analyzed before and after the coagulation.

Secondly, as the key part of the integrated process, ED was used for deep desalination. Before applying the electric potential, feed solution and electric solution in the different compartments were circulated for 30 min. The flow rate was adjusted to prevent a change of the solution volume in different compartments due to water pressure differences among the adjacent compartments. Owning to the high concentration of calcium ions and carbonate ions in the feed solution, ED module was prone to scaling with the generation of calcium carbonate and calcium sulfate. In this way, the pH of solution was adjusted to 6.0 using HCl to ensure that most of the inorganic carbon

was presented as bicarbonate, which will not cause scaling [20]. Desalination of the membrane stack configurations was performed under voltages ranged from 20 to 40 V at room temperature. Every 2 min, electrical conductivity and current density of dilute solution were measured to calculate the total ion-removal efficiency and total energy consumption (EC_{Total}) as well. The total ion-removal rate (η) for the 10-pairs membrane stack can be calculated as follows:

$$\eta = \frac{C_0 - C_t}{C_0} \tag{1}$$

where η is the percentage of ion removal, C_0 and C_t are electrical conductivities of dilute solution at time 0 and t(s), respectively.

The EC_{Total} (not including the energy consumption used in driving solution circulation in the different compartments) of the 10-pairs membrane stack can be calculated as follows:

$$EC_{Total} = \int_0^t \frac{UI}{V} dt \tag{2}$$

where U is the potential (V), I is the current (A), and t is the operation time (h).

Membrane selectivity (S_B^A) represented as membrane separation efficiency, can be calculated as follows [21]:

$$S_B^A = \frac{c_A(t)/c_A(0) - c_B(t)/c_B(0)}{(1 - c_A(t)/c_A(0)) + (1 - c_B(t)/c_B(0))} \tag{3}$$

The range of S_B^A is from −1 to 1. If the ion A transported slower than ion B, the S_B^A value is between 0 and 1. If the ion B transported slower than ion A, the S_B^A value is between −1 and 0.

2.4. Analytical methods

In the whole experiment, all samples were diluted to suitable levels for analysis. The content of cations was decided by AA320N atomic absorption spectrophotometer (Shanghai Precision & Scientific Instrument Co. Ltd); the content of anions was obtained by ion chromatograph (ICS-90 Ion Chromatography System, Dionex). The organic compounds in samples were analyzed using ultraviolet radiation (DU 800UV Spectrometer, Beckman Coulter, Brea, CA) in conjunction with a spectrofluorometer (FluoroMax-4, HORIBA Jobin Yvon, Edison, NJ). COD was quantified with a COD reagent kit (TNT822, Hach Co., Loveland, CO); The BOD_5 was measured by Dilution and Inoculation Method (neq ISO 5815-1). The suspended solid was quantified with Gravimetric Method. Total hardness and total alkalinity were measured using the Ethylenediaminetetraacetic acid Titration Method and Volumetric Method, respectively.

2.5. Membrane fouling analysis

Ion-exchange membrane fouling is one of the major problems that could affect ED process by reducing the flux, increasing the membrane resistance, and energy consumption, as well as decreasing the ions migration rate [20]. Owing to the complex of fracturing wastewater, ion-exchange membranes might be fouled by the organics and suspended solids that barely existed in the product water of coagulation–flocculation. After the experiment, the characteristics of the used CEMs (AEMs) were analyzed using electron microscopy (SEM) and Static Contact Angle. The SEM images of ion-exchange membrane were taken before and after experiments to examine the fouling degree of membranes at 1.50 kV with a scanning electron microscope (SEM: S-4800, Hitachi High-Technologies Corporation, Japan). The contact angle of ion-exchange membrane before and after experiment was measured to further identify the membrane fouling (static contact angle: DSA100, Kruss Corporation, Germany).

3. Results and discussion

3.1. Coagulation–flocculation process

3.1.1. Determination of optimum dosage of coagulant and coagulant aid

Before the studies on the membrane filtration, the optimum dosage of reagents was determined using PAC and PAM as the coagulant and coagulant aid, respectively. The optimum dosages of coagulant and coagulant aid were defined as the value above which there was no significant increase in removal efficiency with further addition of coagulant and coagulant aid [19]. Table 3 shows that the removal efficiency of the COD and turbidity increases with the increase of PAC dosage and nearly levels off at a PAC dosage of 400 mg/L. These results can be explained by the charge density. PAC is a positive charging polyelectrolyte while fracturing wastewater belongs to the emulsion suspension with neutral pH value. Therefore, PAC can easily destabilize the negative charge colloids of emulsion by charge neutralization and adsorption mechanism [22]. When the dosage of PAC is fixed, the removal efficiency of the COD and turbidity is

Table 3
Removal efficiency of COD and turbidity using different dosages of PAC and PAM as coagulant and coagulant aid, respectively

Dosage of PAM (mg/L)		Dosage of PAC (mg/L)				
		120	200	300	400	500
1.5	R_{COD} (%)	59.2	63.6	70.2	76.2	81.3
	$R_{Turbidity}$ (%)	85.5	90.6	99.4	99.5	99.5
3.5	R_{COD} (%)	65.3	72.5	76.6	85.6	87.3
	$R_{Turbidity}$ (%)	89.5	93.2	99.4	99.5	99.5
4.5	R_{COD} (%)	77.8	79.7	83.6	84.5	85.6
	$R_{Turbidity}$ (%)	90.8	95.8	99.8	99.8	99.8
6.5	R_{COD} (%)	79.6	82.5	83.9	86.7	86.1
	$R_{Turbidity}$ (%)	91.0	96.0	99.8	99.8	99.8

improved with the increase of PAM dosage. Even at a low PAM dosage, the addition of PAM leads to a significant increase in efficiency. However, the increase of removal efficiency is not obvious with further addition of PAM when the dosage of PAM is 4.5 mg/L. It can be attributed that PAC can break the emulsion state of fracturing wastewater and the fragile flocs formed by PAC appear rapidly. Based on the bridging mechanism of PAM, the flocs grow fast and precipitation can be easily formed. While there is excessive dosage of PAM and PAC, flocs will break up due to charge reversal and dispersion. Therefore, the optimum dosage of PAM and PAC is 400 and 4.5 mg/L, respectively.

Fig. 2 shows the removal efficiency of the COD and turbidity vs. settling time at the optimum dosage of PAC and PAM. The addition of PAM has a substantial effect on the settling speed when PAC is used as coagulant. After the addition of PAM for 5 min, it is observed that the COD removal rate reaches up to 76% and the turbidity is arranged from the initial value (2,000 NTU) to 24 NTU. This is because PAM favors agglomeration of the flocs formed by the PAC, considerably increasing floc size and settling speed. In that way, the settling time is greatly reduced. After 60 min, the variation of turbidity and COD is not obvious with the settling time prolonged. Therefore, the optimum settling time is 60 min.

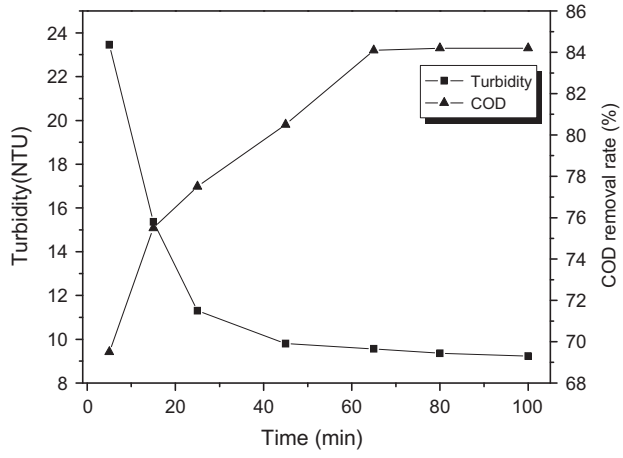

Fig. 2. The influence of standing time on turbidity with the optimum dosage of PAC and PAM.

3.1.2. The quality of product water after the coagulation–flocculation

With the optimum parameters of coagulation–flocculation, the fracturing waste is treated and the quality of product water is shown in Table 4. It can be seen in Table 4 that the organic contaminant has been greatly reduced, especially that the removal rates of the COD, BOD, and the turbidity are 93.4, 94.3, and 99%, respectively. The results indicate that coagulation–flocculation has achieved a better effect and the ED process load is significantly relieved. However, the ion content and the total hardness in the product water are still quite high. Therefore, ED is applied for deep desalination.

3.2. The ED process performance

3.2.1. Characterization of the ED parameters in the circulation experiment

ED process was optimized using the circulation mode to determine the most effective operation conditions. Before determination of the voltage, the circulation operation was experimented to produce a constant stream (ED effluent). Three flow rate 10, 15, and 20 L/h of the effluent are examined in the circulation mode to optimize the effluent salt concentration. The corresponding energy consumptions are 3.802, 3.737, and 3.825 kW h/m^3 when the effluent conductivity is reduced from 22.3 to 1 ms/cm. Therefore, the flow rate of 15 L/h is chosen to produce the whole ED effluent.

In order to determine the optimum voltage, current density, ion-removal rate, and energy consumption are considered in the experiment. Fig. 3 shows the variation of current density as function of time under different voltages. In terms of each curve, the current density gradually decreases as the desalinating time prolongs. This is because the membrane stack resistance increases when the ions are continuously transported from the dilute compartment to concentrated compartment under the direct voltage. According to

Table 4
The main characteristics of product water after coagulation–flocculation

Parameter	Unit	Fracturing wastewater	Water after coagulant
pH		7.0	7.01
Petroleum	mg/L	104	5.4
COD[a]	mg/L	10,873	717
Turbidity	NTU	>2,000	305
BOD_5[b]	mg/L	5,477	15
Suspended solids	mg/L	80	1.6
Total alkalinity	mg/L	1,015	112
Total hardness	mg/L	745	742
Conductivity	ms/cm	22.4	21.1
Chloride	mg/L	6,892	6,086
Nitrate	mg/L	6.3	5.7
Sulfate	mg/L	535	526
Calcium	mg/L	174	162
Magnesium	mg/L	21.7	20.6
Sodium	mg/L	6,055	5,912

[a]COD: chemical oxygen demand.
[b]BOD_5: biochemical oxygen demand at 5 d.

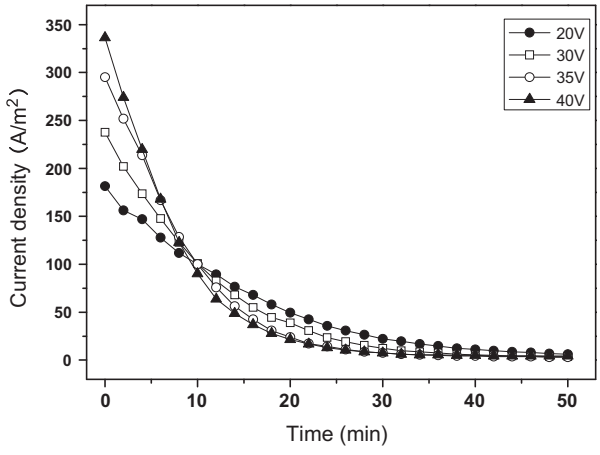

Fig. 3. The current density as a function of time during the operation of the ED with the variation of voltage.

the Ohm's law, the current density decreases with the membrane resistance increasing when the voltage is constant. That is to say, the ratio of the irreversible (the voltage drop or energy used to overcome the electrical resistance) to the reversible contribution to the electric potential becomes bigger with an increasing electrical resistance [20]. The current density is getting higher under a higher voltage in the earlier period of ED (0–10 min). However, the current density corresponding to higher voltage is much lower in the later period of ED (10–50 min). This phenomenon can be attributed to the fact that the current efficiency is much higher with higher voltage in the earlier period of ED and the ions in the dilute compartment are fast reduced to a much lower level. In that way, the membrane stack increases rapidly in the later period of ED and the energy consumption is greatly increased.

The corresponding total ion-removal rate was calculated by Eq. (1) along with the alteration of voltage. As seen in Fig. 4, the total ion-removal rate increases with the desalinating time prolonged and a higher total ion-removal rate can be achieved with a higher voltage just as expected. This is because driving force of ED is DC. Under a higher voltage, ions are rapidly transferred from the desalination compartment to the concentration compartment through the ion-exchange membrane. After 30 min, the ion-removal rate corresponding to 20, 30, 35, and 40 V reached more than 90%. Comparing Fig. 4 with Fig. 5, a higher ion-removal rate and a higher current density can be achieved under a higher voltage, but a higher voltage means that the corresponding energy consumption will be increased. To determine the optimum voltage, the corresponding energy consumptions are investigated when the conductivity the effluent conductivity is reduced from 22.3 to 0.4 ms/cm under different voltages. As seen in Fig. 5, it is observed that the energy consumption increases obviously with the increasing of voltage. When the voltage is 35 V, the corresponding energy consumption is 12.3 kW h/m^3 and total ion-removal rate can reach up to 99.8%. Therefore, the optimum voltage of ED is 35 V.

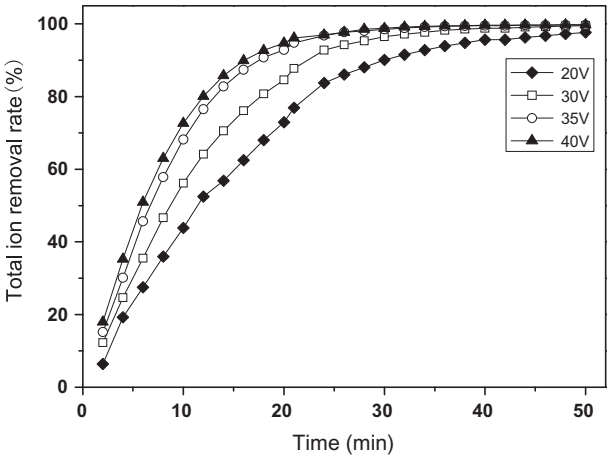

Fig. 4. Total ion-removal efficiency as a function of time during the operation of the ED with the variation of voltage.

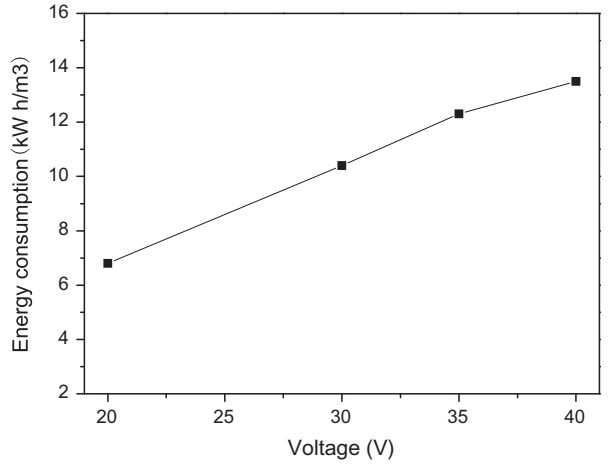

Fig. 5. Energy consumption vs. voltage.

3.2.2. Ion-removal efficiency in the ED experiment

The experiment with circulation mode was applied to desalinate the solution from the coagulant. The ion-removal efficiency as a function of time was studied (pH 5.8–6.0, conductivity 20.1–22.4 ms/cm) when the water conductivity was reduced by 75%. Table 5 compares the ion-removal efficiency of main cations (Ca^{2+}, Na^{+}, and Mg^{2+}) and anions (Cl^{-}, NO_3^{-}, and SO_4^{2-}) by ED. The main cation removal order: $Ca^{2+} > Na^{+} > Mg^{2+}$ and anion removal order: $Cl^{-} > NO_3^{-} > SO_4^{2-}$. This indicates that the AEMs have a better selectivity for NO_3^{-} and Cl^{-} than SO_4^{2-} while CEMs have a better selectivity for Ca^{2+} and Na^{+} than Mg^{2+}, which is a confirmation of a previous study [23]. As shown in Table 5, the removal rate of SO_4^{2-} is only 58.3%, which is much lower than other ion-removal rate. The reason of a lower removal rate of SO_4^{2-} can be attributed to the molar electrical conductivity and hydrated ionic radius. SO_4^{2-} has the largest molar electrical conductivity and the largest hydrated ionic radius as well. The size effect is dominant in this case. Ca^{2+} and Mg^{2+} have the large hydrated ionic radii typical for multivalent ions, and high molar conductivities, thus the mobility is dependent on the applied electrical field. Comparing Ca^{2+} with Mg^{2+}, the latter one has a smaller hydrated ionic radius and a higher molar conductivity, thus Ca^{2+} moves faster. In the experiment, the pH values of diluted and concentrated solutions remain little change, which avoids the electromigration of H^{+} and OH^{-} ions and maintains a high current efficiency.

Table 5
Stokes radius γ_{Stokes}, molar conductivity (λ), and average removal rate (R) of the ions in the experiments

	Cation			Anion		
	Na^{+}	Mg^{2+}	Ca^{2+}	Cl^{-}	SO^{2-}	NO^{3-}
γ_{Stokes} (m)	0.183	0.346	0.308	0.121	0.231	0.129
λ (10^4 Sm^2 mol^{-})	50.1	106.1	119.0	73.6	159.6	71.4
R (%)	74.8	72.5	78.9	73.8	58.3	71.6

Since it is observed that the CEMs exhibit a selectivity for cations and AEMs show a selectivity for anions, the detailed analysis is necessary to investigate how much and to what extent the ions are selectively removed. At the end of ED experiment, the selectivity of Na^{+}/Ca^{2+} is a positive value around 0.01 (data not shown) while the selectivity of Cl^{-}/ SO_4^{2-} is a negative value around −0.07 (data not shown). The results indicate that the Ca^{2+} is selectively transported faster than Na^{+} through CEMs and that SO_4^{2-} is selectively transported slower than Cl^{-} through AEMs. As discussed, higher membrane selectivity means better separation efficiency. The separation efficiency of each ion as function of time during the desalination step at pH 6.0 is shown in Fig. 6. The removal rate of $Ca^{2+}$and Na^{+} are 98.5 and 96.8%, respectively, while the removal rate of Cl^{-} and SO_4^{2-} are 96.8 and 84.3%, respectively. The results are corresponding with the membrane selectivity, which are agreement with the Table 5. It should be noticed that the feed solution is adjusted to a value 6.0 in the experiment, which apparently does not affect the ion selectivity of ion-exchange membrane.

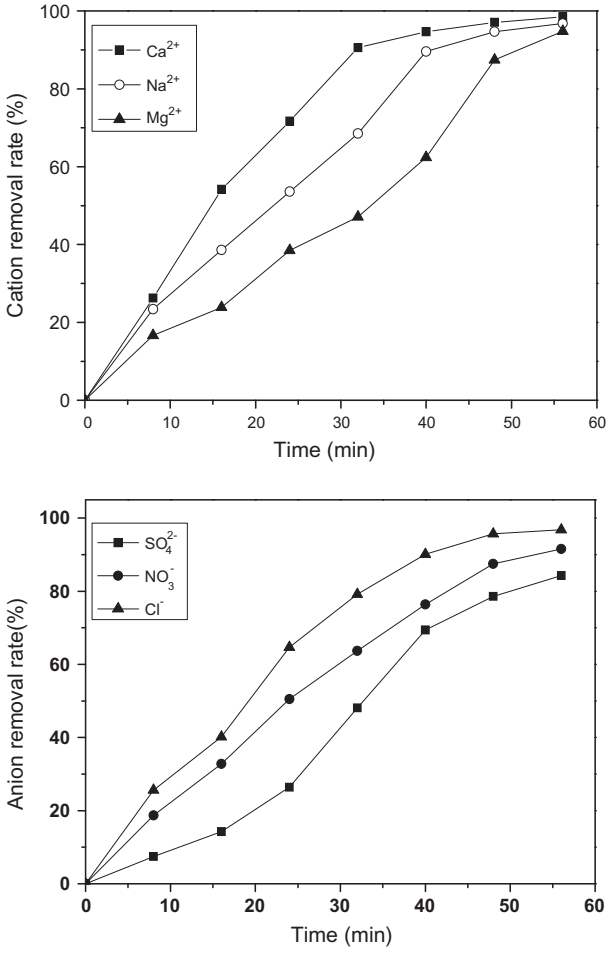

Fig. 6. The influence of time on the removal inorganic ion during ED at pH 6.0.

3.3. The quality of product water after the integrated process

The product water from the integrated process is compared with the quality standard of reclaimed water used for industrial water in China to show the difference of two kinds of water. As shown in Table 6, the organic contaminants of product water from the coagulation have been greatly reduced if compared with the fracturing wastewater. In addition, the mineral ions and the total hardness in product water are greatly reduced. The results indicate that the integrated process can completely resolve the scaling problem in the pipelines. In that way, the fracturing wastewater can be reclaimed efficiently. Therefore, the product water of integrated process can basically meet the requirement of wastewater reclamation except the COD and BOD.

Table 6
comparison of product water from the integrated process and water standard[c]

Parameter	Unit	Product water	Water standard[c]
pH		7.01	6.5–9.5
Petroleum	mg/L	5.4	1
COD[a]	mg/L	717	60
BOD_5[b]	mg/L	305	30
Suspend solids	mg/L	15	30
Turbidity	NTU	1.6	5
Total hardness	mg/L	42	450
Total alkalinity	mg/L	112	350
Chloride	mg/L	219	250
Nitrate	mg/L	0.52	10
Sulfate	mg/L	84	250
Conductivity	ms/cm	0.35	–
Calcium	mg/L	2.6	–
Magnesium	mg/L	1.2	–
Sodium	mg/L	194	–

[a]COD: chemical oxygen demand.
[b]BOD_5: biochemical oxygen demand at 5 d.
[c]The quality standard of reclaimed water used for industrial water in China.

3.4. Ion-exchange membrane fouling analysis and recovery

The membrane performance has an important effect on the system stability and effluent quality by increasing the membrane resistance and energy consumption, as well as decreasing the ions migration yield [23]. In circulation mode, ED runs for 15 h at the voltage of 35 V and flow rate of 15 L/h. After the experiment, the ion-exchange membrane is analyzed. When taking the ED stack apart, no visible fouling deposits are observed on the surface of CEMs, except for a yellow coloration on the AEMs. As further proof, the fouling on membrane surface is identified by SEM as well as Static Contact Angle. As can be seen in Fig. 7, the SEM images show that little change is observed on the surface of CEM, whereas the situation is just opposite for the AEM. To further identify the fouling deposits on the CEMs (AEMs) surface in contact with feed stream, Static Contact Angle is performed on the CEMs (AEMs) before and after ED process and the result is shown in Fig. 8. By comparison, the contact angle of CEM has little change. This indicates that it has a better effect when the pH of feed solution is adjusted to 6 for anti-scaling. However, the contact angle of AEM has an obvious change before and after ED process. This is because the surface of AEM is covered with organic contaminants. In order to prevent the membrane fouling, base cleaning (NaOH) regularly can have a good effect.

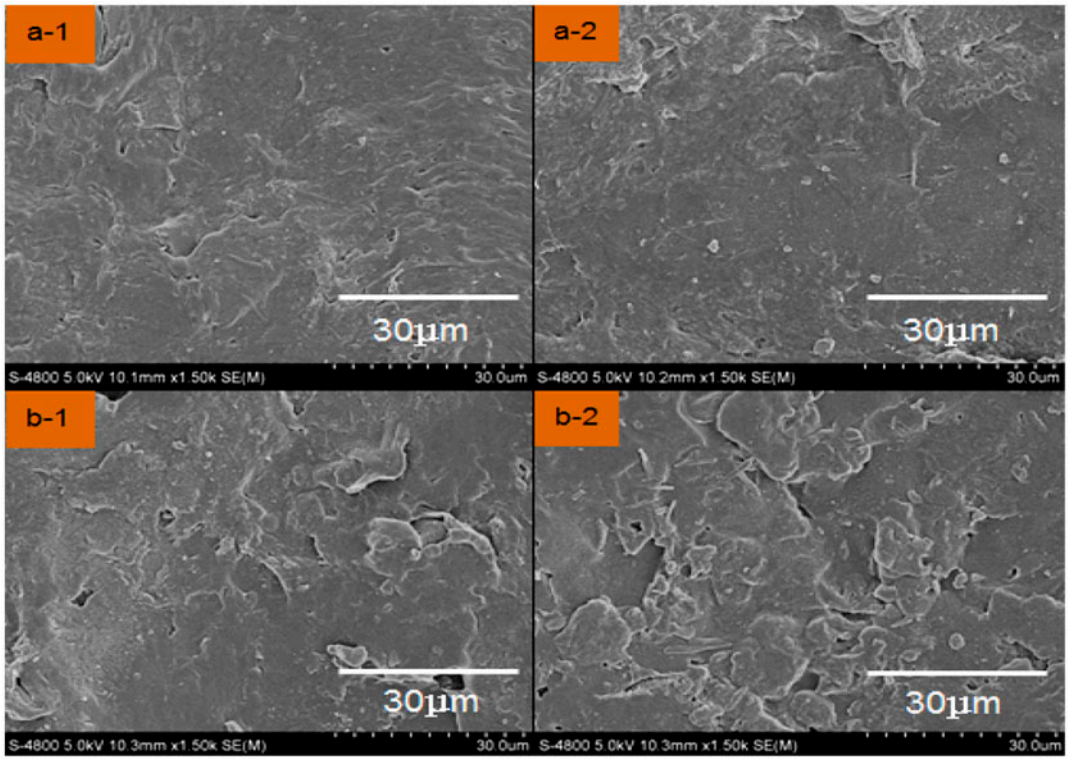

Fig. 7. SEM images (original magnification, 1,500×) of original CEM (a-1), the used CEM (a-2), the original AEM (b-1), and the used AEM (b-2).

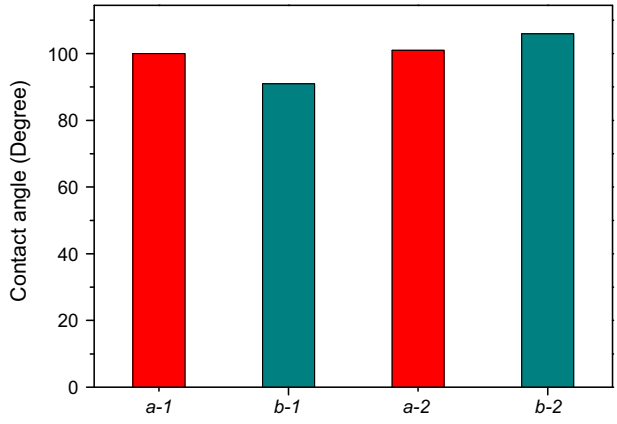

Fig. 8. Contact angle of original CEM (a-1), the used CEM (a-2), the original AEM (b-1), and the used AEM (b-2).

4. Conclusion

In this work, the integrated process consisting of coagulation and ED, has achieved a better effect on treatment of fracturing wastewater. The coagulation of the integrated process sufficiently reduces the organic contaminants, which significantly relieves the load of ED process. It is possible to operate the ED installation under the optimum parameters for a long-term experiment with satisfying desalination effect. Ion-exchange membranes are cleaned by the chemistry method and performance of ion-exchange membrane is basically recovered. In addition, the product water can basically meet the requirement of wastewater reclamation, which is found. A high water recovery (85%) can be achieved by the integrated process. Thus, the integrated process can be technically considered as a good option to treat fracturing wastewater.

Acknowledgments

The authors gratefully acknowledge financial support through the National High Technology Research and Development Program of China (No. 2012AA03A602 and 2012AA021505) and Key Technology Research and Development Program of Qingdao city, Shandong Province, China (No. 12-1-3-56-nsh).

References

[1] M.Y. Soliman, J. Daal, L. East, Fracturing unconventional formations to enhance productivity, J. Nat. Gas Sci. Eng. 8 (2012) 52–67.

[2] W.B. Cai, Z.M. Li, X.L. Zhang, B. Zhang, Q. Zhang, Horizontal well fracturing technology for reservoirs with low permeability, Pet. Explor. Dev. 36 (2009) 80–85.
[3] A. Vengosh, N. Warner, R. Jackson, T. Darrah, The effects of shale gas exploration and hydraulic fracturing on the quality of water resources in the United States, Procedia Earth Planet. Sci. 7 (2013) 863–866.
[4] J.M. Daniel, X.F. Huang, H. Li, K. Sirirat, A. Lee, D. Agnihotri, H. Thomas, R.P. Donald, D.F. Benny, Fouling-resistant membranes for the treatment of flowback water from hydraulic shale fracturing: A pilot study, J. Membr. Sci. 437 (2013) 265–275.
[5] A. Fakhru'l-Razi, A. Pendashteh, L.C. Abdullah, D.R.A. Biak, S.S. Madaeni, Z.Z. Abidin, Review of technologies for oil and gas produced water treatment, J. Hazard. Mater. 170 (2009) 530–551.
[6] K.L. Hickenbottom, N.T. Hancock, N.R. Hutchings, E.W. Appleton, E.G. Beaudry, P. Xu, T.Y. Cath, Forward osmosis treatment of drilling mud and fracturing wastewater from oil and gas operations, Desalination 312 (2013) 60–66.
[7] K.P. Saripalli, M.M. Sharma, S.L. Bryant, Modeling injection well performance during deep-well injection of liquid wastes, J. Hydrol. 227 (2000) 41–55.
[8] L. Gang, S.H. Guo, F.M. Li, Treatment of oilfield produced water by anaerobic process coupled with micro-electrolysis, J. Environ. Sci. 22 (2010) 1875–1882.
[9] R.J. Rosenbauer, J.L. Bischoff, Y.K. Kharaka, Geochemical effects of deep-well injection of the Paradox Valley brine into Paleozoic carbonate rocks, Colorado, U.S.A, Appl. Geochem. 7 (1992) 273–286.
[10] R. Nativ, I. Hemo, G. Weinberger, Injection of industrial wastewater in Israel: Siting criteria for deep injection wells and associated problems, J. Hydrol. 163 (1994) 299–323.
[11] K. Krystyna, B. Michał, R. Mariola, A coagulation-MF system for water treatment using ceramic membranes, Desalination 198 (2006) 92–101.
[12] S. Sinha, Y. Yoon, G. Amy, J. Yoon, Determining the effectiveness of conventional and alternative coagulants through effective characterization schemes, Chemosphere 57 (2004) 1115–1122.
[13] A.M. Lotito, U. Fratino, G. Bergna, C. Di Iaconi, Integrated biological and ozone treatment of printing textile wastewater, Chem. Eng. J. 195–196 (2012) 261–269.
[14] Q.Y. Yue, B.Y. Gao, Y. Wang, H. Zhang, X. Sun, S.G. Wang, R.R. Gu, Synthesis of polyamine flocculants and their potential use in treating dye wastewater, J. Hazard. Mater. 152 (2008) 221–227.
[15] A.I. Zouboulis, N. Tzoupanos, Alternative cost-effective preparation method of polyaluminium chloride (PAC) coagulant agent: Characterization and comparative application for water/wastewater treatment, Desalination 250 (2010) 339–344.
[16] F. Sher, A. Malik, H. Liu, Industrial polymer effluent treatment by chemical coagulation and flocculation, J. Environ. Chem. Eng. 4 (2013) 684–689.
[17] R.K. Nagarale, G.S. Gohil, V.K. Shahi, Recent developments on ion-exchange membranes and electro-membrane processes, Adv. Colloid Interface Sci. 119 (2006) 97–130.
[18] L.T.P. Trinh, Y.J. Lee, J.W. Lee, H.J. Bae, H.J. Lee, Recovery of an ionic liquid [BMIM]Cl from a hydrolysate of lignocellulosic biomass using electrodialysis, Sep. Purif. Technol. 120 (2013) 86–91.
[19] M.I. Aguilar, J. Sáez, M. Lloréns, A. Soler, J.F. Ortuño, V. Meseguer, A. Fuentes, Improvement of coagulation–flocculation process using anionic polyacrylamide as coagulant aid, Chemosphere 58 (2005) 47–56.
[20] Y. Yang, X.L. Gao, A.Y. Fan, L.L. Fu, C.J. Gao, An innovative beneficial reuse of seawater concentrate using bipolar membrane electrodialysis, J. Membr. Sci. 449 (2014) 119–126.
[21] B. Van der Bruggen, A. Koninckx, C. Vandecasteele, Separation of monovalent and divalent ions from aqueous solution by electrodialysis and nanofiltration, Water Res. 38 (2004) 1347–1353.
[22] Y.B. Zeng, C.Z. Yang, J.D. Zhang, W.H. Pu, Feasibility investigation of oily wastewater treatment by combination of zinc and PAM in coagulation/flocculation, J. Hazard. Mater. 147 (2007) 991–996.
[23] Y. Zhang, B. Van der Bruggen, L. Pinoy, B. Meesschaert, Separation of nutrient ions and organic compounds from salts in RO concentrates by standard and monovalent selective ion-exchange membranes used in electrodialysis, J. Membr. Sci. 332 (2009) 104–112.